JACS
JOURNAL OF THE AMERICAN CHEMICAL SOCIETY

Communication

pubs.acs.org/JACS

Determination of the Structural Features of a Long-Lived Electron-Transfer State of 9-Mesityl-10-methylacridinium Ion

Manabu Hoshino,*[,†,‡] Hidehiro Uekusa,[†] Ayana Tomita,[†] Shin-ya Koshihara,[†,‡] Tokushi Sato,[§] Shunsuke Nozawa,[§] Shin-ichi Adachi,[§,∥] Kei Ohkubo,[⊥] Hiroaki Kotani,[⊥] and Shunichi Fukuzumi*[,⊥,#]

[†]Department of Chemistry and Materials Science, Tokyo Institute of Technology, Meguro-ku, Tokyo 152-8551, Japan

[‡]CREST, Japan Science and Technology Agency (JST)

[§]Photon Factory, High Energy Accelerator Research Organization, Tsukuba, Ibaraki 305-0801, Japan

[∥]PRESTO, Japan Science and Technology Agency (JST)

[⊥]Department of Material and Life Science, Graduate School of Engineering, Osaka University, and ALCA, Japan Science and Technology Agency (JST), Suita, Osaka 565-0871, Japan

[#]Department of Bioinspired Science, Ewha Womans University, Seoul 120-750, Korea

Supporting Information

ABSTRACT: Extensive efforts have been devoted to developing electron donor−acceptor systems that mimic the utilization of solar energy that occurs in photosynthesis. X-ray crystallographic analysis shows how absorbed photon energy is stabilized in those compounds by structural changes upon photoinduced electron transfer (ET). In this study, structural changes of a simple electron donor−acceptor dyad, 9-mesityl-10-methylacridinium cation (Acr^+−Mes), upon photoinduced ET were directly observed by laser pump and X-ray probe crystallographic analysis. The *N*-methyl group in Acr^+ was bent, and a weak electrostatic interaction between Mes and a counteranion in the crystal (ClO_4) was generated by photoinduced ET. These structural changes correspond to reduction and oxidation due to photoinduced ET and directly elucidate the mechanism in Acr^+−Mes for mimicking photosynthesis efficiently.

Photosynthesis is an efficient process by which solar energy is utilized for chemical reactions. The profound implication of it is obtained by X-ray crystallographic analysis of structural changes upon photoinduced charge separation in photosynthetic reaction centers, which is the primary process in photosynthesis.[1−3] On the basis of this implication, various electron donor−acceptor molecules have been designed to mimic charge separation processes for use as artificial photosynthetic reaction centers.[4−8] Developing an efficient artificial photosynthetic system is a promising way for solving the problems of global warming and depletion of fossil fuels.[9] However, the short lifetimes of those designed molecules in a photoinduced electron transfer (ET) state have prevented their X-ray crystallographic analysis, which would show how these mimic the charge separation processes in photosynthesis.

Recent X-ray crystallographic studies enabled the observation of structural changes upon photoexcitation.[10−14] Especially, laser pump and X-ray probe crystallography directly provides the three-dimensional (3D) molecular structure of a photoinduced state in a reversible process.[11] In this study, the pump−probe X-ray crystallographic analysis of a donor−acceptor molecule was performed to establish a mechanism for stabilization of the absorbed photon energy by mimicking charge separation.

A donor−acceptor molecule possessing a long ET-state lifetime is suitable for pump−probe crystallography because enough population of the photoinduced ET molecule to detect could be generated in its crystal. Therefore, 9-mesityl-10-methylacridinium perchlorate [Acr^+−Mes(ClO_4^-), **1**] was selected as a target compound. In Acr^+−Mes, an electron donor, mesitylene (Mes), and an acceptor, 10-methylacridinium cation (Acr^+), are directly connected to each other.[15] Despite the close proximity of Acr^+ and Mes, there is no π conjugation between them because of the orthogonal geometry. Scheme 1a shows photoinduced generation of the ET state of Acr^+−Mes ($Acr^{\bullet}$−$Mes^{\bullet+}$). Because of this geometrical feature and the high energy of $Acr^{\bullet}$−$Mes^{\bullet+}$ (2.37 eV), which lies deep in the Marcus-inverted region,[16] back-ET to the ground state becomes extremely slow at low temperatures, so the ET state has a long lifetime in frozen media (e.g., 2 h at 203 K).[15,17] However, the formation of such a long-lived ET state of Acr^+−Mes has been questioned in light of the alternative formation of the locally excited triplet state of the Acr^+ moiety.[18,19]

The crystal structure of **1** in the photoinduced state was determined by a pump−probe X-ray diffraction experiment in which X-ray pulses (width = 100 ps) and a femtosecond laser excitation pulse were synchronized at a frequency of 946 Hz at beamline PF-AR NW14A.[20] Because 9-phenyl-10-methylacridinium perchlorate [Acr^+−Ph(ClO_4^-), **2**] does not undergo photoinduced ET and its lowest photoexcited state is the locally excited singlet state of Acr^+ (Scheme 1b),[21] it was used as a reference compound. The samples were cooled to 90 K by a cold nitrogen stream. Experimental details are described in the Supporting Information (SI). Figure 1 shows the obtained structures.[22]

Received: January 19, 2012
Published: March 1, 2012

   dx.doi.org/10.1021/ja300602h | *J. Am. Chem. Soc.* 2012, 134, 4569−4572

Scheme 1. Photoinduced Processes in (a) Acr^+−Mes and (b) Acr^+−Ph

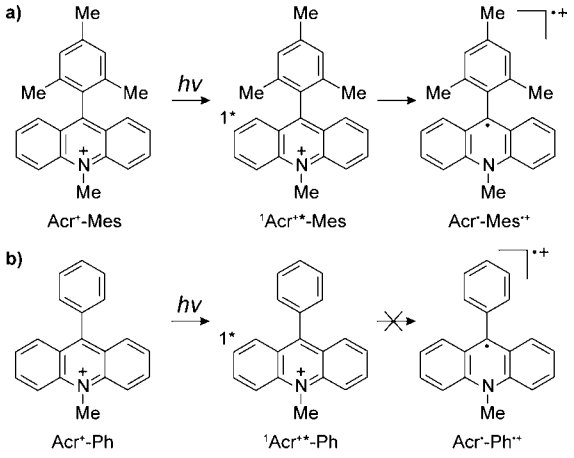

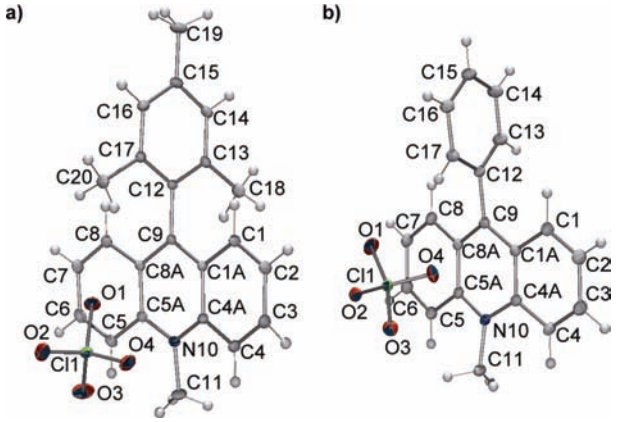

Figure 1. ORTEP diagrams of (a) **1** and (b) **2** in the light-off condition (50% thermal ellipsoids).

No significant geometrical difference was observed between the averaged structures of **1** obtained with the light on (i.e., the pump−probe condition) and off (i.e., the dark condition) (Table S1 in the SI). This indicates that the population of a photoinduced species generated in **1** is too small to be observed by typical crystallographic analysis. Therefore, the photoinduced difference (photodifference) Fourier map, in which the difference of the observed structural factors in the light-on and -off stages [$F_{o(on)} - F_{o(off)}$] is used as the coefficient,[23] was drawn (Figure 2a). The noise density level of this map was defined as ±0.11 e Å^{-3} by drawing the difference Fourier map using two data sets of F_o under light-off conditions. The heating effect of photoirradiation is negligible in this map (details are described in the SI). Therefore, only the photoinduced change is precisely reflected in this map. A pair of positive and negative electron densities in the map corresponds to slight movement of an atom by photoexcitation.[24] Thus, the electron densities around C11 can be assigned to bending of the *N*-methyl group upon photoirradiation. Its bending angle was 10.3(16)°; in other words, C11 moved 0.27(4) Å away from the mean plane containing N10, C4A, and C5A. The map also indicates photoinduced movement and rotation of ClO_4^-. Cl1 moved a distance 0.144(8) Å. On the other hand, the intramolecular twist from the orthogonal to the coplanar geometry in Acr^+−Mes, reported in similar compounds,[25] was not observed in the

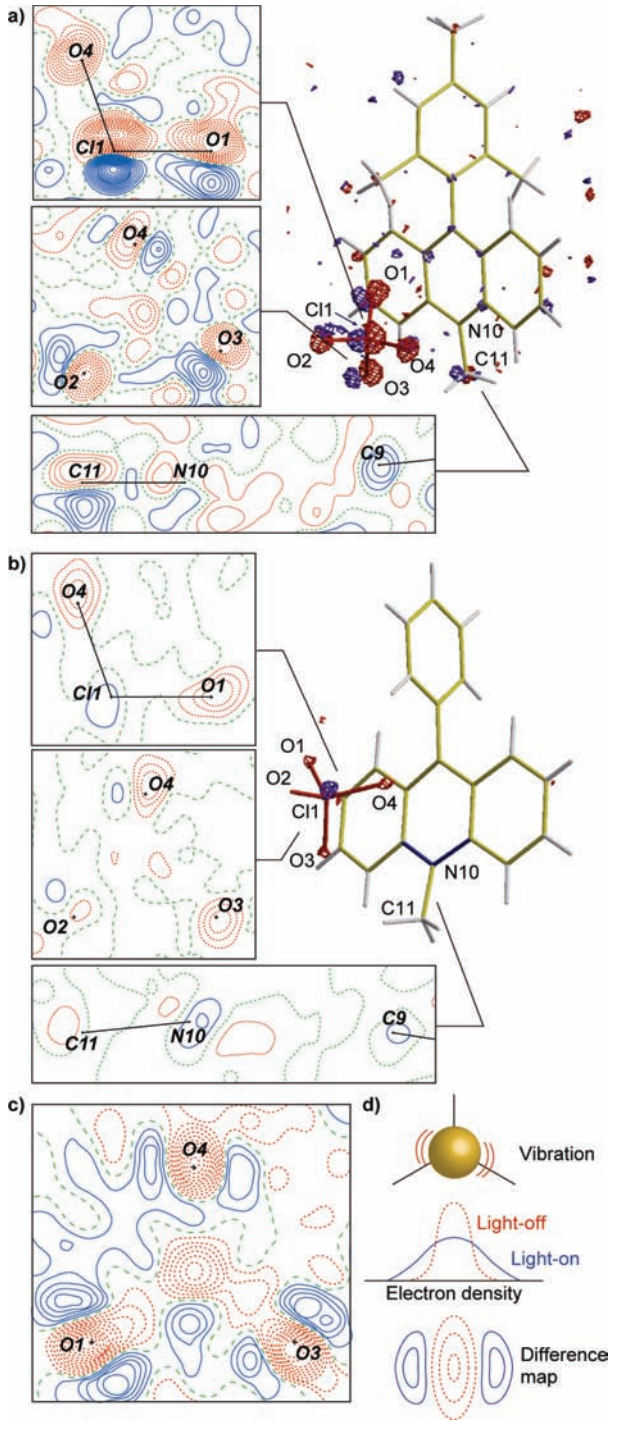

Figure 2. (a, b) 2D and 3D photodifference Fourier maps of (a) **1** and (b) **2** with a contour interval of 0.03 e Å^{-3} and ±0.1 e Å^{-3} isosurfaces. (c) 2D map for **2** with contour intervals of 0.01 e Å^{-3}. In the 2D maps, blue solid, red dotted, and green dashed lines denote positive, negative, and zero electron densities, respectively, while in the 3D maps, purple and red surfaces denote positive and negative electron densities, respectively. (d) Schematic drawing of thermal vibrations (as a result of atomic vibrations, the electron density in the light-on state is elongated in the vibration direction).

photodifference Fourier map. Structural analysis revealed that the population of the photoinduced molecule in **1** is ca. 2%.

The crystal structure of **2** in the photoinduced state was also determined by a pump−probe X-ray diffraction experiment.

dx.doi.org/10.1021/ja300602h | *J. Am. Chem. Soc.* 2012, 134, 4569−4572

Just as for **1**, no geometrical difference between the average structures of **2** in the light-on and -off stages was observed (Table S2). However, unlike for **1**, no significant change in the electron density was observed around Acr^+−Ph and only small regions of negative electron density were observed near ClO_4^- in its photodifference Fourier map (Figure 2b). The map around ClO_4^-, which has rather fine contours, reveals that regions of negative electron density are surrounded by regions of positive electron density (Figure 2c). This is characteristic of the difference electron density attributed to atomic or molecular thermal vibrations. Hence, the geometrical change that occurs on the generation of the excited singlet state of **2** is smaller than the slight vibrations due to thermal deactivation. Because the excited singlet state is generated by an electron transition in only the Acr^+ moiety, the geometrical change by generation of the singlet excited state in Acr^+−Mes may be identical to the change in Acr^+−Ph. On the basis of these considerations, the observed change in the difference Fourier map of **1** is ascribed to the generation of the ET state of Acr^+−Mes.

Natural population analysis[26] of Acr^+ and $Acr^\bullet$ indicated an increase in the electron occupancy of the $2p_z$ natural atomic orbital (NAO) for the nitrogen atom (+0.11625) upon one-electron reduction of Acr^+. Natural bonding orbital (NBO) analysis[27] revealed that this population increased as a result of filling of the lone-pair NBO of the nitrogen atom, which is vacant in the ground state, with rearrangement ofthe valence electrons by reduction. The lone pair electrostatically repels the *N*-methyl bonding electrons, enhancing the nitrogen's sp^3 hybrid orbital character to induce bending of the *N*-methyl group that produces a pyramidal geometry around the nitrogen atom. In contrast with the case of $Acr^\bullet$, NAO and NBO analyses of the excited triplet state of the Acr^+ moiety reduced the population of the nitrogen $2p_z$ NAO (−0.05038). This indicates that generation of the excited triplet state does not induce bending of the *N*-methyl group.

Figure 3a depicts the reaction cavities around the *N*-methyl group and ClO_4^-; these indicate a free space for the selected group to move in the crystal.[28] Thus, the *N*-methyl group bends in the sterically favorable direction in **1**, and the geometry around the nitrogen atom becomes pyramidal because there is more space for the *N*-methyl group to deform in the observed bending direction than in the opposite direction. However, the reaction cavity around ClO_4^- indicates that the photoinduced geometrical change of ClO_4^- is sterically unfavorable because O1 moves out of the reaction cavity. Such a sterically unfavorable geometrical change must result from cooperative geometrical rearrangement in the crystal. The bending of the *N*-methyl group by ET enlarges the cavity around ClO_4^-. Consequently, O1 can move toward that enlarged space. In fact, the bending and moving directions are the same (Figure 3b). Moreover, the closest Mes from ClO_4^- is positioned in the direction of movement of Cl1. This suggests that ClO_4^- is moved with rotation by the $Mes^{\bullet+}\cdots ClO_4^-$ electrostatic interaction in the photoinduced state of **1**. Thus, the observed bending of the *N*-methyl group and the movement of ClO_4^- provide strong evidence for the generation of the ET state of Acr^+−Mes.

The reproducibility of the photoinduced geometrical changes in **1** was confirmed by analyzing diffraction data obtained under continuous photoirradiation (see the SI). Although the electron density change based on those data was smaller than that obtained in the pump−probe experiment because of the lower excitation photon density from the light source (a xenon lamp was used), it had the same characteristics as that in the pump−probe experiment (Figure 4). It should be noted that the photoinduced structural changes in **1** disappeared immediately when the excitation light source was turned off. Because $Acr^\bullet$−$Mes^{\bullet+}$ has a very long lifetime, $Acr^\bullet$−$Mes^{\bullet+}$ is easily saturated in **1**. In fact, the photoinduced cooperative geometrical change of ClO_4^- (Figure 3b) requires the formation of at least two $Acr^\bullet$−$Mes^{\bullet+}$ around one ClO_4^- (one creates the space by causing the

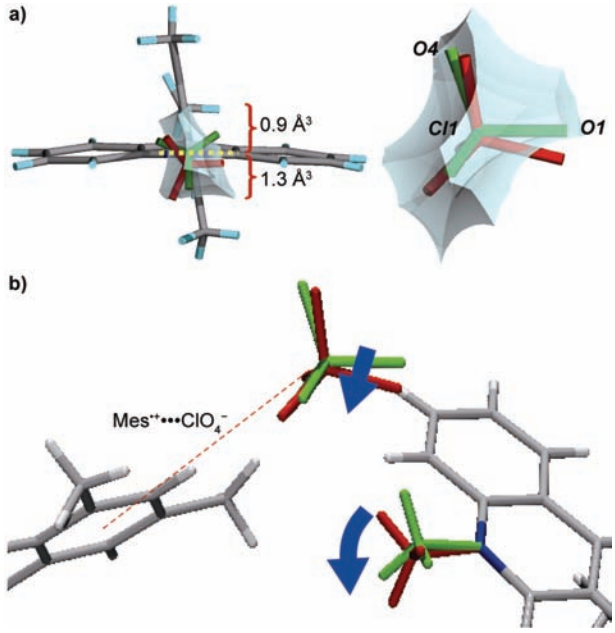

Figure 3. (a) Drawing of the reaction cavity (greenish-blue area): (left) drawing around the *N*-methyl group viewed along C11−N10, with numbers indicating the volumes of the divided cavity formed by the yellow dotted line; (right) drawing around ClO_4^-. (b) Cooperative photoinduced geometrical changes. Fragments of the ground- and ET-state mlecules are colored greenish-yellow and red, respectively. The red dashed line indicates the suggested $Mes^{\bullet+}\cdots ClO_4^-$ electrostatic interaction.

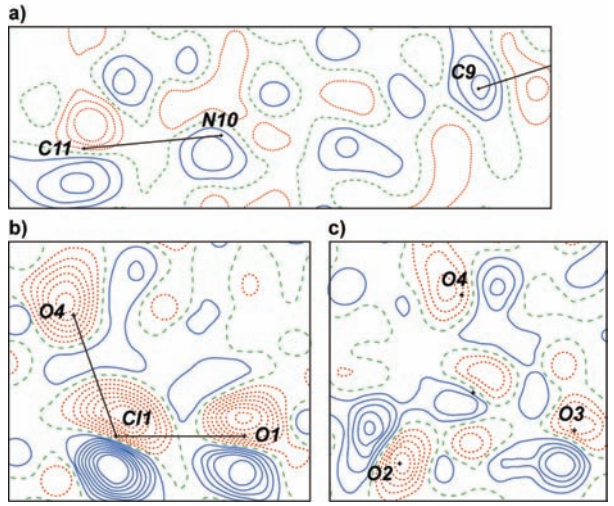

Figure 4. 2D maps corresponding to (a) bending of the *N*-methyl group, (b) movement of ClO_4^-, and (c) rotation of ClO_4^-. The contour interval is 0.01 e $Å^{-3}$, and the colors have the same meanings as Figure 2a−c.

dx.doi.org/10.1021/ja300602h | *J. Am. Chem. Soc.* 2012, 134, 4569−4572

N-methyl group to bend and the other provides electrostatic attraction), suggesting the generation of domains of $Acr^{\bullet}$–$Mes^{\bullet+}(ClO_4^-)$ in **1**. In such domains, bimolecular back-ET between the long-lived ET molecules[29] is not negligible. Therefore, despite the use of pump–probe X-ray diffraction, only 2% of the $Acr^{\bullet}$–$Mes^{\bullet+}$ could be detected.

In conclusion, the generation and structural features of the ET state of Acr^+–Mes were directly observed by pump–probe X-ray diffraction and crystal structure analysis. The observed bending of the *N*-methyl group clearly reflected the formation of a lone pair on N10 and the enhancement of its sp^3 character by ET. We also characterized the photoinduced cooperative geometrical rearrangement in **1** by drawing the reaction cavity. This cooperative change indicates domain formation by long-lived ET molecules. On the other hand, the intramolecular twist between Acr^+ and Mes was not accompanied by the generation of the ET state. This explains the restriction of intramolecular back-ET by electronic coupling between $Acr^{\bullet}$ and $Mes^{\bullet+}$. This study provides definitive proof for the formation of a long-lived ET state with its structural features and establishes the concept of designing an efficient artificial photosynthetic reaction center, paving the way for the development of useful artificial photosynthetic systems.

■ ASSOCIATED CONTENT

Supporting Information

Experimental procedures, supporting figures and tables, complete ref 20, and a CIF. This material is available free of charge via the Internet at http://pubs.acs.org.

■ AUTHOR INFORMATION

Corresponding Author

mhoshino@chem.titech.ac.jp; fukuzumi@chem.eng.osaka-u.ac.jp

Notes

The authors declare no competing financial interest.

■ ACKNOWLEDGMENTS

This work was partially supported by Grants-in-Aid for JSPS Fellows and Scientific Research (to M.H.), a Grant-in-Aid (20108010 and 23750014) and a Global COE Program, "The Global Education and Research Center for Bio-Environmental Chemistry" (to S.F. and K.O.) from MEXT, Japan, and NRF/MEST of Korea through the WCU (R31-2008-000-10010-0) and GRL (2010-00353) Programs (to S.F.). This work was approved by the Photon Factory Program Advisory Committee (PF-PAC 2009G626). We thank Prof. Y. Ohashi (Tokyo Tech) and Prof. S. Nanbu (Sophia University) for fruitful discussions.

■ REFERENCES

(1) Wöhri, A. B.; Katona, G.; Johansson, L. C.; Fritz, E.; Malmerberg, E.; Andersson, M.; Vincent, J.; Eklund, M.; Cammarata, M.; Wulff, M.; Davidsson, J.; Groenhof, G.; Neutze, R. *Science* **2010**, *328*, 630.

(2) Katona, G.; Snijder, A.; Gourdon, P.; Andréasson, U.; Hansson, O.; Andréasson, L.-E.; Neutze, R. *Nat. Struct. Mol. Biol.* **2005**, *12*, 630.

(3) Stowell, M. H. B.; McPhillips, T. M. *Science* **1997**, *276*, 812.

(4) Wasielewski, M. R. *Acc. Chem. Res.* **2009**, *42*, 1910.

(5) Gust, D.; Moore, T. A.; Moore, A. L. *Acc. Chem. Res.* **2009**, *42*, 1890.

(6) Fukuzumi, S. *Phys. Chem. Chem. Phys.* **2008**, *10*, 2283.

(7) Guldi, D. M.; Rahman, G. M. A.; Sgobba, V.; Ehli, C. *Chem. Soc. Rev.* **2006**, *35*, 471.

(8) Harriman, A.; Sauvage, J.-P. *Chem. Soc. Rev.* **1996**, *25*, 41.

(9) Lewis, N. S.; Nocera, D. G. *Proc. Natl. Acad. Sci. U.S.A.* **2006**, *103*, 15729.

(10) Hoshino, M.; Uekusa, H.; Ishii, S.; Otsuka, T.; Kaizu, Y.; Ozawa, Y.; Toriumi, K. *Inorg. Chem.* **2010**, *49*, 7257.

(11) Coppens, P.; Benedict, J.; Messerschmidt, M.; Novozhilova, I.; Graber, T.; Chen, Y.-S.; Vorontsov, I.; Scheins, S.; Zhang, S.-L. *Acta Crystallogr., Sect. A* **2010**, *66*, 179.

(12) Pillet, S.; Legrand, V.; Weber, H.-P.; Souhassou, M.; Létard, J.-F.; Guionneau, P.; Lecomte, C. *Z. Kristallogr.* **2008**, *223*, 235.

(13) Cole, J. M. *Acta Crystallogr., Sect. A* **2008**, *64*, 259.

(14) Collet, E.; Lemée-Cailleau, M.-L.; Cointe, M.-L.; Cailleau, H.; Wulff, M.; Luty, T.; Koshihara, S.; Meyer, M.; Toupet, L.; Rabiller, P.; Techert, S. *Science* **2003**, *300*, 612.

(15) Fukuzumi, S.; Kotani, H.; Ohkubo, K.; Ogo, S.; Tkachenko, N. V.; Lemmetyinen, H. *J. Am. Chem. Soc.* **2004**, *126*, 1600.

(16) Marcus, R. A.; Sutin, N. *Biochim. Biophys. Acta* **1985**, *811*, 265.

(17) Fukuzumi, S.; Kotani, H.; Ohkubo, K. *Phys. Chem. Chem. Phys.* **2008**, *10*, 5159.

(18) Benniston, A. C.; Harriman, A.; Li, P.; Rostron, J. P.; van Ramesdonk, H. J.; Groeneveld, M. M.; Zhang, H.; Verhoeven, J. W. *J. Am. Chem. Soc.* **2005**, *127*, 16054.

(19) Ohkubo, K.; Kotani, H.; Fukuzumi, S. *Chem. Commun.* **2005**, 4520.

(20) Nozawa, S.; et al. *J. Synchrotron Radiat.* **2007**, *14*, 313.

(21) Ohkubo, K.; Suga, K.; Fukuzumi, S. *Chem. Commun.* **2006**, 2018.

(22) Crystallographic information files (CIFs) for all of the crystal structures were submitted to The Cambridge Crystallographic Data Centre (CCDC) under reference numbers 818662–818667.

(23) Carducci, M. D.; Pressprich, M. R.; Coppens, P. *J. Am. Chem. Soc.* **1997**, *119*, 2669.

(24) Kim, C. D.; Pillet, S.; Wu, G.; Fullagar, W. K.; Coppens, P. *Acta Crystallogr., Sect. A* **2002**, *58*, 133.

(25) (a) Hu, J.; Xia, B.; Bao, D.; Ferreira, A.; Wan, J.; Jones, G. II; Vullev, V. I. *J. Phys. Chem. A* **2009**, *113*, 3096. (b) Jones, G. II; Yan, D.; Hu, J.; Wan, J.; Xia, B.; Vullev, V. I. *J. Phys. Chem. B* **2007**, *111*, 6921.

(26) Reed, A. E.; Weinstock, R. B.; Weinhold, F. *J. Chem. Phys.* **1985**, *83*, 735.

(27) Foster, J. P.; Weinhold, F. *J. Am. Chem. Soc.* **1980**, *102*, 7211.

(28) Ohashi, Y.; Yanagi, K.; Kurihara, T.; Sasada, Y.; Ohgo, Y. *J. Am. Chem. Soc.* **1981**, *103*, 5805.

(29) Murakami, M.; Ohkubo, K.; Nanjo, T.; Souma, K.; Suzuki, N.; Fukuzumi, S. *ChemPhysChem* **2010**, *11*, 2594.